Ultrafast Evolution of the Excited States in the Chlorophyll a/b Complex CP29 from Green Plants Studied by Energy−Selective Pump−Probe Spectroscopy †

ARTICLE *in* BIOCHEMISTRY · FEBRUARY 1998

Impact Factor: 3.02 · DOI: 10.1021/bi9722655 · Source: PubMed

Ultrafast Evolution of the Excited States in the Chlorophyll *a/b* Complex CP29 from Green Plants Studied by Energy-Selective Pump−Probe Spectroscopy†

Claudiu C. Gradinaru,*,‡ Andy A. Pascal,§ Frank van Mourik,‡ Bruno Robert,§ Peter Horton,|| Rienk van Grondelle,‡ and Herbert van Amerongen‡

Department of Physics and Astronomy and Institute for Condensed Matter Physics and Spectroscopy, Free University of Amsterdam, De Boelelaan 1081, 1081 HV, Amsterdam, The Netherlands, Section de Biophysique des Protéines et des Membranes, DBCM/CEA & URA 2096/CNRS CE-Saclay, F-91191 Gif-sur-Yvette, France, and Robert Hill Institute, Department of Molecular Biology and Biotechnology, University of Sheffield, Sheffield S10 2UH, United Kingdom

Received September 10, 1997; Revised Manuscript Received November 6, 1997

ABSTRACT: The energy transfer process in the minor light-harvesting antenna complex CP29 of green plants was probed in multicolor transient absorption experiments at 77 K using selective subpicosecond excitation pulses at 640 and 650 nm. Energy flow from each of the chlorophyll (Chl) *b* molecules of the complex could thus be studied separately. The analysis of our data showed that the "blue" Chl *b* (absorption around 640 nm) transfers excitation to a "red" Chl *a* with a time constant of 350 ± 100 fs, while the 'red' Chl *b* (absorption at 650 nm) transfers on a picosecond time scale (2.2 ± 0.5 ps) toward a "blue" Chl *a*. Furthermore, both fast (280 ± 50 fs) and slow (10 −13 ps) equilibration processes among the Chl *a* molecules were observed, with rates and associated spectra very similar to those of the major antenna complex, LHC-II. Based on the protein sequence homology between CP29 and LHC-II, a basic modelling of the observed kinetics was performed using the LHC-II structure and the Förster theory of energy transfer. Thus, an assignment for the spectral properties and orientation of the two Chl's *b*, as well as for their closest Chl *a* neighbors, is put forward, and a comparison is made with the previous assignments and models for LHC-II and CP29.

Considerable effort has been expended in recent years to investigate energy transfer occurring in plants and photosynthetic bacteria prior to its chemical conversion at the reaction center (*1*). In photosystem II (PSII) of higher plants and green algae, the reaction center is surrounded by several chlorophyll binding integral proteins that efficiently absorb and funnel the solar energy. Two complexes, CP43 and CP47, bind only Chl[1] *a* and *β*-carotene (no Chl *b* is present) and are tightly attached to the reaction center. The light-harvesting function is performed mainly by the outer chlorophyll *a/b* (LHC) binding proteins, of which LHC-II (also known as LHCIIb) plays the major role, binding about 65% of PSII Chl. A model for the organization of LHC-II was proposed recently, based on electron crystallography on two-dimensional crystals (*2*). The quasi-atomic resolution (3.4 Å) allowed the mapping of 2 carotenoid (Car) molecules in central positions, assumed to be luteins, surrounded by 12 chlorophylls in each monomeric unit of the trimers. However, a clear distinction between Chl *a* and Chl *b*, or between Q_x and Q_y directions within single pigments, could not be made. Also, as concluded from biochemical data, approximately two Chl's and one Car are not resolved in the structure. Since triplets are formed mainly on Chl *a* molecules, it was argued that the nearest seven porphyrins to the central luteins must be Chl *a*, to match the requirement for efficient triplet quenching.

There are at least three other (minor) LHC proteins associated with PSII, called CP29, CP26, and CP24 (or Lhcb4−6, respectively), that bind all together only about 15% of PSII chlorophyll (*3*, *4*). They contain relatively high amounts of xantophylls, particularly violaxanthin, that is presumably involved in regulation of the energy flow to and from the reaction center (*5*). This process, known as nonphotochemical quenching (q_E), is inhibited by dicyclohexylcarbodiimide (DCCD), which was found to bind both to CP29 and to CP26 (*6*, *7*). The involvement of the minor antennae in controlling the energy level is further supported by their intermediate location between the major LHC-II complex and the PSII core region (*3*, *4*, *8*). The largest protein of the LHC family, CP29, has at least 262 amino acids and an apparent molecular mass of 29 kDa. The cofactors, as determined from chemical analysis (HPLC), are probably 6 Chl *a* and 2 Chl *b* per protein and 2−3 Car's, namely, 1 lutein, 1 violaxanthin, and close to 1 neoxanthin (*7*, *9*−11). Although no direct structural information is available for CP29, due to the sequence homology with LHC-II it is expected to form a similar fold with three membrane-

† C.C.G. was supported by Grant 1932802 from the Human Frontier Science Program Organisation. A.A.P. was a receiptient of a FEBS post-doctoral fellowship.

* Corresponding author. Telephone: (+31) 20 4447942: Fax (+31) 20 4447899. E-mail: klaus@nat.vu.nl.

‡ Free University of Amsterdam.

§ DBCM/CEA & URA 2096/CNRS CE-Saclay.

|| University of Sheffield.

[1] Abbreviations: Chl, chlorophyll; LHC, light-harvesting complex; DCCD, dicyclohexylcarbodiimide; HPLC, high-pressure liquid chromatography; SE, stimulated emission; ESA, excited state absorption; SADS, species-associated difference spectrum.

S0006-2960(97)02265-4 CCC: $15.00
Published on Web 01/06/1998

spanning helices plus a short amphiphatic helix at the lumenal side. All but one of the identified Chl binding sites in LHC-II are conserved (*3, 7*), so the Chl molecules in CP29 are probably positioned as in Figure 1A. A reconstitution study showed that the CP29 protein scaffold can accommodate different chromophores, with one Chl *a* that can be replaced by one Chl *b* depending on the initial conditions (*9*). Photoinhibitory conditions induce reversible phosphorylation of the complex at the stromal side, affecting the spectroscopic properties (*10, 11*).

The object of this study is the excited state dynamics in the CP29 complex on a (sub)picosecond time scale and its structural implications. In light of the general resemblance of the conformation of the Chl *a/b* binding proteins, the conclusions are extended to the bulk complex. Since LHC-II can be easily purified and a structural model is available, it was extensively studied in search for a straightforward relationship between organization and function. Steady-state spectroscopy revealed the existence of 9−11 Chl Q_y (0−0) bands in a relatively small spectral domain (630−690 nm), almost matching the number of pigments per monomeric unit (*12*). The excited state kinetics, investigated by several groups in transient absorption or fluorescence up-conversion experiments, are characterized by an ultrafast Chl *b*−Chl *a* transfer occurring in three time windows ($\lesssim$200 fs, ∼500 fs, and 2−6 ps) and a spectral equilibration among Chl *a* molecules with time constants of $\lesssim$300 fs, 2−4 ps, and 10−20 ps (*13*−18). Ascribing various spectral or kinetic features proved to be a very difficult task given the lack of important structural details, such as precise identity and orientation of the chlorophylls, or the absence of a high degree of spatial symmetry.

Conversely, CP29 and all other minor LHC proteins show lower complexity, due to a smaller amount of bound chromophores, and the data may thus prove more easily interpretable. However, problems concerning isolation in sufficient amounts hindered not only their crystallization but also extensive spectroscopic analysis. CP29 isolated by nondenaturating isoelectric focusing has been the subject of a basic spectroscopic analysis (*19*). Our preparation was obtained by cation exchange chromatography and exhibited similar spectral characteristics (*20, 21*). The most distinctive feature is the presence of two separate bands in the low-temperature absorption spectra at 638 and 650 nm ascribed to the two Chl's *b* identified in the chemical analysis. Thus, by investigating the energy transfer pattern upon selective excitation of each of these two chlorophylls, we can in principle discriminate between different rates and their associated spectra. Then, in the frame of the sequence homology and of the model for LHC-II structure, a direct link between structure and dynamics can be performed.

MATERIALS AND METHODS

Sample Preparation. The basic protocol used for isolating CP29 complex from PSII spinach was previously described by Henrysson *et al*. (*20*). A new version of this procedure was used to obtain our preparation, as described elsewhere (*21*). In short, the complex was purified from Tris-washed PSII membranes by HPLC fractionation on a cation-exchange column equilibrated with a buffer containing 0.1% (w/v) sulphobetaine SB12 and 0.05% (w/v) dodecyl maltoside (DM). Two successive chromatography runs yielded sufficiently purified CP29 in milligram quantities. The homogeneity was tested by a combination of SDS/urea polyacrylamide gel electrophoresis and immunological analysis. Pigment analysis revealed the existence of six Chl *a* and two Chl *b* molecules and equal amounts (∼0.65) of lutein, neoxanthin, and violaxanthin per complex (*21*). For experiments, the protein was solubilized in 0.06% (w/v) DM, 80% (v/v) glycerol, and 20 mM HEPES, at pH 7.5. Cuvettes with a path length of 2 mm were used. All measurements were performed at 77 K in a liquid nitrogen cryostat (Oxford Instruments, DN1704). The OD in the 674 nm peak was approximately 0.8/mm for all the pump−probe experiments.

Laser System. The transient absorption data were recorded with subpicosecond resolution using the same spectrophotometer as in (*22*). A synchronously-pumped double dye-jet laser (Model Satori 774 by Coherent) produces pulses with approximately 200 fs duration at an energy of the order of 1 nJ. These pulses are amplified up to about 0.5 mJ in a three-stage dye amplifier pumped at 30 Hz by a regenerative amplifier (RGA/PTA60 from Continuum), with a good stability (noise less than 10% rms). The low repetition rate ensured the absence of accumulating Chl *a* triplet states at 77 K. Excitation pulses at 640 and 650 nm were selected from the white light continuum using interference filters (6−7 nm FWHM) and then amplified in a single dye cell (DCM). The probing light was generated in a sapphire plate, divided into a probe and a reference beam, and projected onto two separate diode arrays. Both beams were polarized under magic angle (54°45′) relative to the vertically polarized pump beam. Excitation pulses of ∼0.3 μJ, focused on a spot of ∼0.3 mm diameter in the sample, resulted in bleaching in less than 20% of the CP29 complexes. We used delays between pump and probe pulses up to 200 ps, divided in 96 steps. One dataset was the result of averaging more than 300 shots for each delay position, and 4 datasets were recorded for both 640 and 650 nm excitation. The spectra were detected over a wavelength window spanning from 630 to 695 nm, with 0.5 nm resolution. The instrument response of the setup at all wavelengths was about 320 fs, as determined from the rise of induced birefringence in CS2. The absorption changes in the Chl *b* region were around 50 mOD, whereas the noise level was on the order of 1 mOD. Absorption spectra of the CP29 sample taken before and after the measurements proved to be identical.

Data Analysis. The time-gated spectra were analyzed using a global fitting routine as described previously (*23*). Datasets for the same excitation wavelength were fitted together in an irreversible sequential model with four or five lifetimes, yielding species-associated difference spectra (SADS). The instrument response function, fitted with a gaussian, had in all cases full width at half-maximum (FWHM) values of 200−250 fs, slightly lower than determined from the CS_2 signal. This difference was taken into account by fixing the FWHM of the instrument response to several values between 200 and 320 fs in the fitting program. The main outcome was an imprecision in determining the fastest lifetime, which is included in the error margins given below. The wavelength dependence of the location of time zero was fitted in the CS_2 data with a polynomial function and then applied as a fixed parameter in the analysis of CP29 data.

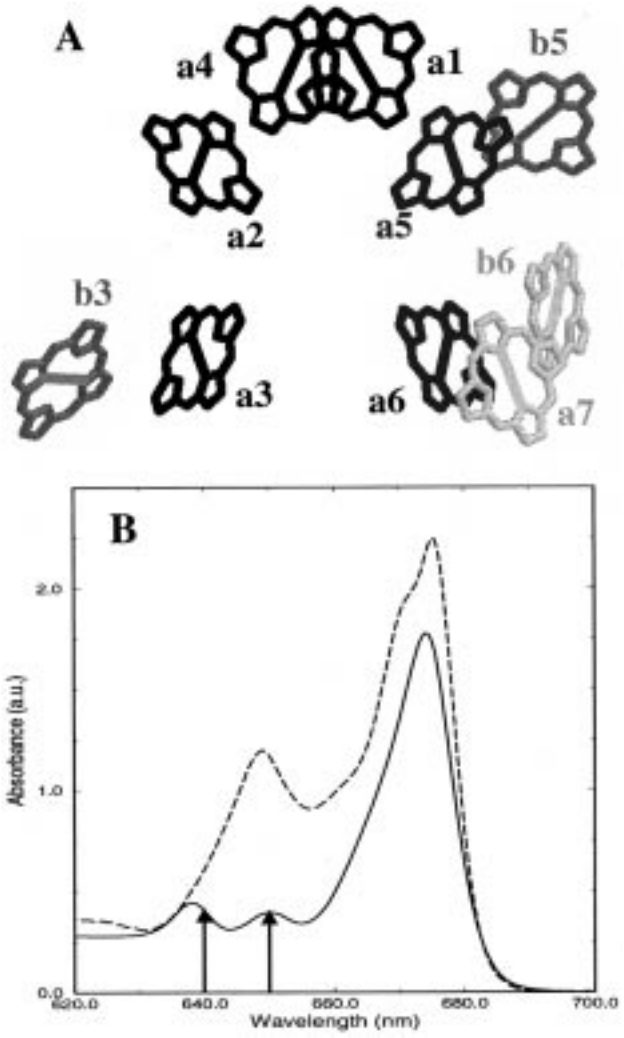

FIGURE 1: (A) LHC-II chlorophylls presumably present in CP29, based on protein sequence homology. Arrangement, assignment, and notation as in (*2*). Chl *a*, black; Chl *b*, grey; some uncertain pigments, light grey. The lines are connecting the atoms NB and ND within each molecule (see text). (B) 77 K absorption spectra of CP29 (solid) and LHC-II (dashed) recorded with 0.5 nm bandwidth. The arrows indicate the excitation wavelengths used in this study.

RESULTS

The 77 K absorption spectrum of the CP29 sample used in the pump−probe measurements is shown in Figure 1B. For comparison, the spectrum of LHC-II is also presented. Obvious diminution of the Chl *a* band at 670 nm and of the Chl *b* band at 650 nm can be noticed, in line with the reduction of pigment content in CP29 as compared to LHC-II (6 Chl *a* *vs* 8 Chl *a* and 2 Chl *b* *vs* 6 Chl *b*, respectively).

First we will focus on the excited state dynamics upon excitation around 650 nm. Transient absorption difference spectra recorded at various delays after the excitation pulse are shown in Figure 2. Already within the pulse duration about half of the total bleaching/stimulated emission (SE) is at wavelengths longer that 660 nm. In the first picosecond, the amount of bleaching/SE around 650 nm remains mostly unchanged, whereas in the Chl *a* region the signal around 675 nm increases at the expense of the decrease observed in the area below 670 nm. Around 1.5 ps delay, the bleaching/SE at the pumping wavelength starts to decrease, and after

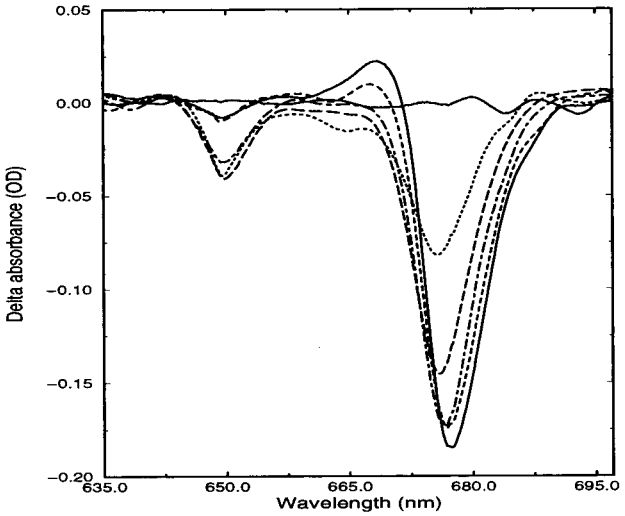

FIGURE 2: Transient absorption difference spectra measured upon excitation at 650 nm for different delays: before $t = 0$ (solid), 250 fs (dotted), 500 fs (long dashed), 1.5 ps (dot−dashed), 10 ps (dashed), and 60 ps (solid).

10 ps, most of it has disappeared, while the amplitude of the main Chl *a* bleaching has further increased and has shifted to the red. At longer time intervals, the bleaching/SE of Chl *a* equilibrates toward the low-energy states, whose amplitudes do not decay on the time scale of our experiment.

These time-gated spectra were analyzed globally, and a minimum of four lifetimes were required for a good fit: 280 fs, 2.2 ps, 10.5 ps, and 1 ns (Figure 3). The quality of the fit was judged from a χ^2 test on the residuals and from their temporal and spectral distribution. To illustrate the spectral evolution, we used a model with four consecutive states, irreversibly decaying one into the next: A → B → C → D. This means that state A, which is formed by the excitation pulse within the instrument response time, decays with a time constant τ_A into state B, which in turn decays into state C with a longer time constant τ_B. Then state C will evolve with an even longer time constant τ_C into the last state D, which returns to the ground state with the lifetime τ_D. Note that the absence of uphill energy transfer at 77 K allows us to treat these steps as irreversible. One should keep in mind that at least some of these lifetimes might not be true eigenvalues of the complex and the associated spectra (SADS) do not necessarily correspond to real states. The first SADS (Figure 3A) grows within the response time of the setup (330 fs), thus serving as bleaching/SE at time zero. Maxima are found at 650.5 and 674.5 nm, and a small shoulder is present around 660 nm. About 60% of the total bleaching/SE resides on Chl *a* molecules, a fraction comparable to the Chl *a* contribution in the OD spectrum around 650 nm. Hence, upon direct excitation, ultrafast vibrational and/or electronic relaxation of Chl *a* takes place within the duration of the pulse. The next SADS (Figure 3B) arises from the preceding state with a time constant of 280 fs. The most striking change consists of the simultaneous decrease of bleaching/SE between 655 and 673 nm and the build up of the signal above 675 nm. No major alteration of the Chl *b* bleaching can be noticed. The development of the third SADS (Figure 3C) from the previous spectrum takes place with a lifetime of about 2.2 ps. Here we only see the transfer of excitation from around 650 nm to Chl *a* molecules showing bleaching/SE that peaks now slightly to the red, at

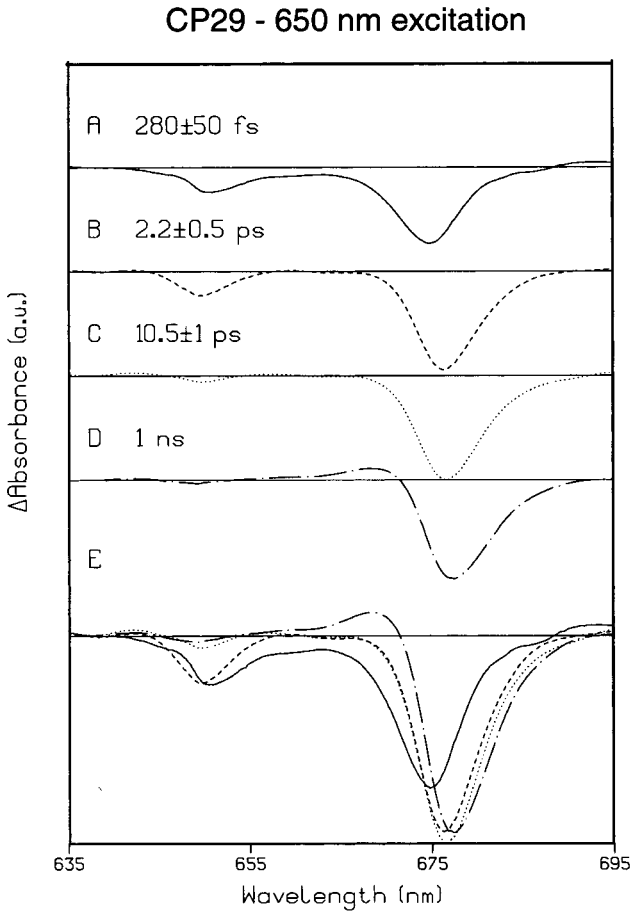

FIGURE 3: Results of the global analysis of data in Figure 2, using a sequential model with four states irreversibly decaying one into the next (A → B → C → D). The SADS and the related lifetimes are depicted in panels A−D (see text). In panel E, an overlay of all the spectra is shown.

676.5 nm. The end spectrum (Figure 3D) is formed with a time constant of 10.5 ps and consists of a bleaching/SE maximum at 677.5 nm, excited state absorption (ESA) features at 669 and 660 nm, and a small residual bleaching around 650 nm. A relatively slow equilibration process (10−20 ps) between blue and red chlorophylls *a* has been observed before in low-temperature studies on LHC-II (*13*, *16*, *18*). The decay time of the last SADS could not be accurately determined, since our datasets extended to delays up to 200 ps, and it was fixed to 1 ns in the fitting program. The error margins for the other lifetimes were estimated from various restrictions on the analysis that did not produce significant changes on the associated spectra, and also not on the statistical distribution of the residuals.

Some characteristic transient spectra recorded upon exciting the Chl *b* that absorbs around 640 nm are shown in Figure 4. One can see the bleaching/SE growing within the pulse duration mainly at 640 nm and throughout the Chl *a* absorption region and, to a small extent, around 650 nm. Direct excitation of Chl *a* either in the Q_y vibrational side band or in the Q_x band leads, as for 650 nm pumping, to a significant amount of Chl *a* bleaching/SE even at very early delays. In addition, the red wing of the pump spectrum excites a minor fraction of the Chl *b* absorbing at 650 nm. This gives us the opportunity to study simultaneously the energy transfer from the two distinct Chl *b* molecules of CP29. Most of the bleaching/SE centered at 639 nm decays

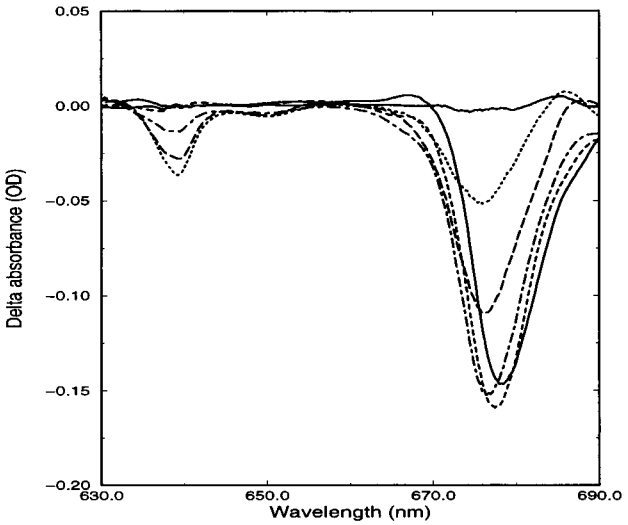

FIGURE 4: Transient difference spectra measured upon 640 nm excitation for the following delays: before $t = 0$ (solid), 200 fs (dotted), 500 fs (long dashed), 1 ps (dot−dashed), 10 ps (dashed), and 100 ps (solid).

in less than 1 ps, whereas the signal around 650 nm takes picoseconds to disappear. Corresponding to these decays, ingrowths of the bleaching/SE and small red shifts of the maximum are detected in the Chl *a* domain.

The spectral evolution described above was found to be satisfactorily characterized by 4 time constants, with the related SADS being displayed in Figure 5. As expected from absorption contributions around 640 nm, about 55% of the total bleaching/SE belongs to Chl *a* in the instantaneous SADS (Figure 5A). This spectrum shows peaks at 639 and 676 nm plus a small shoulder around 650 nm. This initial state undergoes a fast (∼350 fs) evolution to a state that lives about 2.5 ps. In the new state (Figure 5B), more bleaching/SE on Chl *a* is observed (maximum at 677 nm) at the expense of a large decrease of the signal around 640 nm. The 2.5 ps lifetime is remarkably similar to the rate of energy transfer from Chl *b* occurring upon excitation at 650 nm (*vide infra*). Restriction of the fit to a confined spectral region around 650 nm was needed to unveil this small kinetic component, otherwise split up between the fast and slow processes. Indeed, we can clearly see the minor bleaching at 650 nm disappearing when the next SADS sets in (Figure 5C), and its decay-associated spectrum resembles the one found for 650 nm excitation (spectra not shown). Also similar to the previous set of data, a slow spectral equilibration among different Chl *a* takes place with a time constant of about 12.5 ps toward a state (Figure 5D) that shows maximum bleaching/SE at 678 nm. Comparing the areas of bleaching/SE of the final *vs* initial state, after corrections for ESA and different extinction coefficients for Chl *b* and Chl *a*, we estimate that the annihilation level was at most 10% for both pump wavelengths.

DISCUSSION

In the present study, we report for the first time rates and associated spectra of ultrafast energy transfer in a minor antenna complex, i.e., CP 29. Table 1 shows a summary of lifetimes that were resolved by our analysis *vs* the ones that resulted from multiple kinetic experiments on LHC-II. The intricate singlet energy transfer in the bulk complex can be

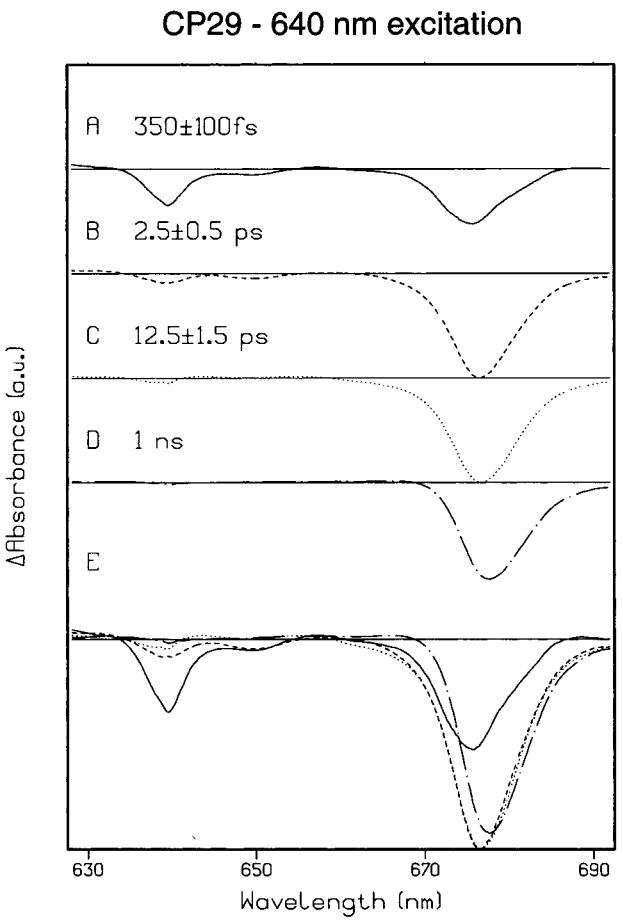

FIGURE 5: SADS and their lifetimes as resulted from the global analysis of the data described in Figure 4 (A−D). Panel E shows an overlay of all the spectra A−D.

Table 1: Summary of the Energy Transfer Processes in CP29 *vs* LHC-II[a]

τ (ps)	from (nm)	to (nm)
0.35 ± 0.05 (0.3, 1)	640 (Chl *b*)	678 (Chl *a*)
2.2 ± 0.5 (≲0.2, ∼0.5, 2−6)	650 (Chl *b*)	670−676 (Chl *a*)
0.28 ± 0.05 (0.3−0.4)	660−670 (Chl *a*)	670−680 (Chl *a*)
10−13 (10−20)	∼670 (Chl *a*)	∼678 (Chl *a*)

[a] The values for the LHC-II lifetimes, given in parentheses, are as in (*13*−*18*).

projected onto a set of many exponential decays, with time constants ranging from less than a few hundreds of femtoseconds to some tens of picoseconds. This distribution of rates is in general agreement with the structural data, since the nearest-neighbor distances and/or mutual orientations are not uniform. The purpose of the experiments presented here was to concentrate on some of these processes, particularly on the multiexponential Chl *b*−Chl *a* transfer, since CP29 binds only two Chl *b* molecules with distinct spectroscopic features.

We found that direct excitation followed by ultrafast vibrational relaxation taking place in less than 200 fs localizes an important amount of excitations (≳ 50%) on Chl *a* before energy transfer from Chl *b* sets in. We did not detect "blue" Chl *a* as intermediates in the transfer pathway from Chl *b* to "red" Chl *a*, but both fast (250−300 fs) and slow (10−13 ps) spectral equilibration processes occurred among the Chl *a* molecules in CP29. These values are very similar to the time constants seen for LHC-II (see Table 1), probably reflecting a high resemblance in pigment organization in the two complexes. This also indicates that the observed energy transfer occurs predominantly within monomeric LHC-II, so the aggregation state (trimers or monomers) does not significantly influence the ultrafast dynamics, as concluded in (*24*). For a well-coupled functioning complex, the long-living spectrum should be independent of excitation wavelength. Although the end spectra for the two pump wavelengths exhibit very similar characteristics (position of the maximum, amplitude, width), the small features observed for 650 nm excitation around 650 and 670 nm may be due to some unbound pigments (Figure 3D and 5D). In both cases, the level of singlet−singlet annihilation was low, with some very small effects on the 2.2 ps and 10−13 ps processes only.

By pumping around 640 nm, we mainly study the energy flow from the "blue" Chl *b* (absorption maximum at 638 nm). The decay of initial bleaching/SE on this chromophore was found to be satisfactorily fit with a single exponential, having a lifetime of 350 ± 100 fs. The energy is transferred from this Chl *b* to a relatively "red" Chl *a*, showing bleaching/SE at wavelengths longer than 675 nm. A similar rate was found in a 12 K transient absorption study on the LHC-II complex, upon selective excitation at 640 nm (*16*). The energy transfer from the other Chl *b* molecule present in CP29 (absorption maximum at 650 nm) is relatively slow, with a time constant of 2.2 ± 0.5 ps. Transfer times larger than 1 ps have been observed before in several experiments on LHC-II, such as one- and two-color pump−probe (2−6 ps) or anisotropy decay (∼5 ps). The contribution of this process to the total Chl *b*−Chl *a* energy transfer was found to be in the range of 20%, and, accordingly, one out of the five Chls *b* identified in the structure would be responsible for it *(13)*. Note that a kinetic component exhibiting remarkable similarity (both spectral and temporal) was resolved upon excitation around 640 nm. Our data also show that the "red" Chl *b* in CP 29 is paired with a Chl *a* absorbing just above 670 nm.

Förster-type incoherent energy transfer forms the usual theoretical frame for modelling the data obtained so far from ultrafast spectroscopy on LHC-II. The coherence effects in the energy transfer from Chl *b* to Chl *a* (energetically separated by more than 500 cm^{-1}) are expected to be small, since the estimated excitonic dipole coupling probably does not exceed 100 cm^{-1}. Thus, we will consider localized excitations that hop between a donor (D) and an acceptor (A) separated by a distance *R* in a medium of refractive index n, with a rate given by the formula:

$$k_{DA} = \frac{C}{n^4}(\kappa^2/R^6)$$

Here κ^2 is a geometrical factor with values between 0 and 4, depending on the mutual orientation of the two molecules, and *C* is a factor that contains the radiative lifetime of the donor and the overlap-integral of donor emission and acceptor absorption. As calculated by Visser *et al.* (*13*) for the low-temperature transfer in LHC-II, the values for *C* were 18 nm^6 ps^{-1} and 14 nm^6 ps^{-1} for transfer from the Chl *b* absorbing at 650 and 640 nm, respectively. The refractive index *n* was allowed to be a free parameter in the modelling. Moreover, the ratio τ_{650}/τ_{640}, where the dependence on *n* is

Table 2: Values for the κ^2 Factor for the Chl *b*−Chl *a* Pairs in CP29[a]

#*b*, #*a*	*R* (nm)	AC−AC	AC−BD	BD−AC	BD−BD
*b*3, *a*3	0.92	**0.233**	**0.431**	1.309	0.507
*b*5, *a*5	0.89	1.049	**0.022**	0.082	**1.086**

[a] In this table we compare the geometrical factors κ^2 for the two Chl *b*−Chl *a* pairs for all four possible orientations. AC indicates that the Q_y transition is along the NA−NC, and BD that the Q_y dipole is perpendicular to that, i.e., along the NB−ND axis. The left position in the first column is associated with Chl *b*, the right position with Chl *a*. *R* is the distance between the Mg atoms of the Chl's and is given in nanometer. Boldfaced values correspond to orientations that are in contradiction with the present assignment from LHC-II (*25, 26*).

cancelled out, was used for comparison with experiment rather than the individual values. In the following, we will use the pigment assignment and notation as in Kühlbrandt *et al.* (*2*), where each Chl molecule can have two possible orientations for the Q_y transition dipole moment: either along NA and NC, or along NB and ND (notations NA, NB, NC, and ND refer to the nomenclature of the nitrogen atoms in the porphyrin rings in the crystal structure). Despite the fact that the CP29 protein sequence for spinach has not been published, the high degree of sequence homology across species for those organisms where it was determined (*3, 7*) allows us to make certain assumptions with respect to the spinach sequence. In addition, the spectroscopic features of CP29 from spinach are almost identical to those reported before for the other organisms. Since the only proposed Chl *b* binding residues conserved in CP29 as compared to LHC-II are the ones for *b*3 (His 212) and *b*5 (Glu 139), we assume that the two Chl *b* molecules in the former complex are at these two positions (see Figure 1A). Note that the binding residues for *b*1 and *b*2 were not identified in the LHC-II structure.

Both *b*3 and *b*5 molecules have a neighboring Chl *a* molecule that is by far the closest, *a*3 and *a*5, respectively. The distances and the geometrical factors κ^2 for these two Chl *b*−Chl *a* pairs for all orientations of the Q_y dipole moments are listed in Table 2. If we assume that *b*3 is responsible for the 650 nm absorption band and take into account all possible mutual orientations of the Q_y dipoles, it follows that the *b*3 Q_y transition should be oriented along the NA−NC axis (AC for short) for the ratio τ_{650}/τ_{640} to match the observed values. However, this orientation for *b*3, also needed to explain the negative sign of the linear dichroism (LD) at 650 nm in CP29 (*21*), is not consistent with the previous assignment for LHC-II (*b*3 along the NB−ND axis, or BD for short), as in (*25*). Therefore, we tested the other possibility, with *b*3 assigned to the pigment absorbing around 640 nm. Orientation along the BD axis was demanded in order to account for the observed positive LD at this wavelength (*19, 21*). Then, only two possible configurations for the *b*5−*a*5 pair (*b*5 along AC and *a*5 along BD, or *b*5 along BD and *a*5 along AC) could yield an appropriate ratio τ_{650}/τ_{640}. However, only the second solution is in agreement with the orientation proposed for *a*5 in LHC-II (along AC axis), based on LD restrictions (*25, 26*). It is not possible to unequivocally decide about the orientation of *a*3, although BD gives a slightly better ratio τ_{650}/τ_{640} than AC (4 *vs* 11), plus a more reasonable value for the refractive index in the Förster rates (1.5 *vs* 1.9).

On the other hand, it was argued that *b*6 instead of *b*5 might be present in CP29, based on biochemical studies (*11*). If this is the case, the only possible assignment that is in accordance with the observed kinetics would be *b*3 (orientation BD) at 638 nm, *a*3 (AC) around 676 nm, *b*6 (AC) at 650 nm, and *a*6 (AC) around 672 nm, with a refractive index $n \approx 1.6$. However, for the AC orientation, *b*6 would not produce a negative LD around 650 nm, as observed in the measured spectrum (*19, 21*). This assignment is further disfavored by the finding that the q_E inhibitor DCCD specifically binds to the residue Gln 166 (the presumed binding site for *b*6) but leaves the spectroscopic properties of the CP29 complex unchanged (*7*).

In conclusion, both ultrafast energy transfer and linear dichroism of CP29 lead to the following spectral and spatial assignment: *b*3 (BD orientation) at 638.5 nm, *a*3 (BD or AC) around 676 nm, *b*5 (BD) at 650 nm, and *a*5 (AC) around 672 nm. Given the organization of the pigments in Chl *b*−Chl *a* pairs, the possible absence of *a*7 (or any other Chl *a* but *a*3 and *a*5) in CP29 does not affect the rates of energy transfer from *b*3 or *b*5. Hence, the lifetimes observed in CP29 probably correspond to similar processes observed in LHC-II, and in that case our assignment can be extended to the latter complex. Previous spectral assignments of the two Chl *b* molecules investigated in this study endorsed the opposite case, i.e., *b*3 absorbing at 650 nm and *b*5 at 640 nm (*10, 27*). However, our solution agrees well with the outcome of modelling the transfer kinetics in LHC-II in (*13*) where it was concluded that either *b*1 or *b*5 is responsible for the picosecond component in the Chl *b*−Chl *a* transfer.

ACKNOWLEDGMENT

Dr. Ulrich Wacker and Dr. Klaus D. Irrgang are kindly acknowledged for their work during the isolation procedure. We thank Dr. Ivo H. M. van Stokkum for help concerning the data analysis.

REFERENCES

1. Van Grondelle, R., Dekker, J. P., Gillbro, T., and Sundström, V. (1994) *Biochim. Biophys. Acta 1187*, 1−65.
2. Kühlbrandt, W., Wang, D. N., and Fujiyoshi, Y. (1994) *Nature 367*, 614−621.
3. Jansson, S. (1994) *Biochim. Biophys. Acta 1184*, 1−19.
4. Dainese, P., and Bassi, R. (1991) *J. Biol. Chem. 266*, 8136−8142.
5. Ruban, A. V., Young, A. J., Pascal, A. A., and Horton, P. (1994) *Plant Physiol. 104*, 227−234.
6. Walters, R. G., Ruban, A. V., and Horton, P. (1994) *Eur. J. Biochem. 226*, 1063−1069.
7. Pesaresi, P., Sandonna, D., Giuffra, E., and Bassi, R. (1997) *FEBS Lett. 402*, 151−156.
8. Camm, E. L., and Green, B. R. (1989) *Biochim. Biophys. Acta 974*, 180−184.
9. Giuffra, E., Cugini, D., Croce, R., and Bassi, R. (1996) *Eur. J. Biochem. 238*, 112−120.
10. Croce, R., Breton, J., and Bassi, R. (1996) *Biochemistry 35*, 11142−11148.
11. Testi, M. G., Croce, R., Polverino-De Laureto, P., and Bassi, R. (1996) *FEBS Lett. 399*, 245−250.
12. Nüssberger, S., Dekker, J. P., Kühlbrandt, W., Bolhuis, B. M., van Grondelle, R., and van Amerongen, H. (1994) *Biochemistry 33*, 14775−14783.
13. Visser, H. M., Kleima, F. J., van Stokkum, I. H. M., van Grondelle, R., and van Amerongen, H. (1996) *Chem. Phys. 210*, 297−312; Visser, H. M., Kleima, F. J., van Stokkum, I. H. M., van Grondelle, R., and van Amerongen, H. (1997) *Chem. Phys. 21*5, 299.

14. Connelly, J. P., Müller, M. G., Hucke, M., Gatzen,G., Mullineaux, C. W., Ruban, A. V., Horton, P., and Holzwarth, A. R. (1997) *J. Phys. Chem. B 101*, 1902−1909.
15. Du, M., Xie, X., Mets, L., and Fleming, G. R. (1994) *J. Phys. Chem. 98*, 4376−4741.
16. Bittner, T., Wiederrecht, G. P., Irrgang, K.-D., Renger, G., and Wasielewski, M. (1995) *Chem. Phys. 194*, 312−322.
17. Pållson, L. O., Sprangfort, M. D., Gulbinas, V., and Gillbro, T. (1994) *FEBS Lett. 339*, 134−138.
18. Kwa, S. L. S., van Amerongen, H., Lin, S., Dekker, J. P., van Grondelle, R., and Struve, W. S. (1992) *Biochim. Biophys. Acta 1101*, 202−212.
19. Zuchelli, G., Dainese, P., Jennings, R. C., Breton, J., Garlaschi, F. M., and Bassi, R. (1994) *Biochemistry 33*, 8982−8990.
20. Henrysson, T., Schröder, W. P., Spangfort, M., and Åkerlund, H.-E. (1989) *Biochim. Biophys. Acta 977*, 301−308.
21. Pascal, A. A., Gradinaru, C. C., Wacker, U., Peterman, E. J. G., Calkoen, F., Irrgang, K., Horton, P., van Grondelle, R., Robert, B., and van Amerongen, H., unpublished results.
22. Visser, H. M., Groot, M.-L., van Mourik, F., van Stokkum, I. H. M., Dekker, J. P., and van Grondelle, R. (1995) *J. Phys. Chem. 99*, 15304−15309.
23. Van Stokkum, I. H. M., Scheer, T., Brouwer, A. M., and Verhoeven, J. W. (1994) *J. Phys. Chem. 98*, 852−866.
24. Kleima, F. J., Gradinaru, C. C., Calkoen, F., van Stokkum, I. H. M., van Grondelle, R., and van Amerongen, H. (1997) *Biochemistry 36*, 15262−15268.
25. Gülen, D., van Grondelle, R., and van Amerongen, H. (1995) in *Photosynthesis: from Light to Biosphere. Proceedings of the Xth International Photosynthesis Conference* (Mathis, P., Ed.) Vol. I, p 335, Kluwer Academic Publishers, Dordrecht.
26. Gülen, D., van Grondelle, R., and van Amerongen, H. (1997) *J. Phys. Chem. B 101*, 7256−7261.
27. Van Amerongen, H., van Bolhuis, B. M., Betts, S., Mei., R., van Grondelle, R., Yocum, C. F., and Dekker, J. P. (1994) *Biochim. Biophys. Acta 1188*, 227−234.

BI9722655